

Interactive comment on “Factors controlling the community structure of picoplankton in contrasting marine environments” by Jose Luis Otero-Ferrer et al.

Jose Luis Otero-Ferrer et al.

jootero@uvigo.es

Received and published: 14 September 2018

Anonymous Referee 1 Referee comments shown in black, Author replies shown in blue, Changes to manuscript in red

Overall comments

The manuscript investigates the relationship between nutrient supply estimated by measurements of turbulent mixing and nitrate gradients and the community structure of picophytoplankton (including both autotrophic and heterotrophic groups). The take-home message of the work is that studies that use ambient nutrient concentrations as

C1

a proxy of nutrient availability could be misleading as in many regions of the ocean the supply of nutrients by turbulent diffusion is not registered in bottle samples of nutrients. This is an important message that needs to be communicated to the wider marine science community.

The manuscript is well written and provides a nice overview of the ecological literature of marine picophytoplankton. The dataset of turbulent mixing, nitrate concentrations and picoplankton community structure is novel and covers a variety of hydrographic and trophic regimes.

I have a few questions and comments concerning both the estimation of nutrient supply using combined MSS and nutrient profiles and the choice of sampling stations used in the analysis which I hope the authors may be able to address.

Specific comments

1) NUTRIENT FLUX ESTIMATES

Although the authors correctly point out that concomitant datasets of turbulent mixing and picophytoplankton community structure are rare, this may be due in part to the lack of high-quality estimates of nutrient flux from microstructure profile measurements in the surface ocean with coincident depth-resolved nutrient profiles (required to obtain a robust estimate of the nutrient gradient near the nutricline). The vertical resolution of the nutrient profiles within the dataset is unclear (only a range between 3 and 9 depths is provided, but it could be tricky to use 3/4 depths to provide a good estimate of the nutrient gradient). Could the extent of the density gradient be over/underestimated in cases where the depth resolution is low and by how much? It would be good to have a frequency histogram for the dataset showing the number of depths per profile so the reader is aware of the vertical resolution of nutrient concentrations across the dataset.

We agree with the reviewer that the lower vertical resolution of nitrate concentration in comparison to turbulent data incorporates some uncertainty, which is very hard to

C2

evaluate, in the calculation of nitrate diffusive fluxes. Lower vertical resolution (5 ± 2 sampling depths) was used in the shallower stations sampled in the Galician coastal upwelling, whereas in the deeper NW Mediterranean and the tropical and subtropical regions we used 7 ± 1 and 11 ± 2 depths, respectively. The text has been modified and a new figure (Figure A2.A) has been included in the supplementary material, to represent the frequency histogram of sampling depths used to compute the nitrate vertical gradient in each region. The maximum sampling depth where the microstructure turbulence profiler was deployed is now indicated in Table 1.

Original Page 5 – Line 11-13 Samples for the determination of nitrate (NO_3) + nitrite (NO_2) were collected from 3 to 9 depths in rinsed polyethylene tubes and stored frozen at -20°C until analysis on land, according to standard methods using the automated colorimetric technique (Grasshoff et al., 2007).

Modified to Page 5 – Line 21-26 Samples for the determination of nitrate (NO_3) + nitrite (NO_2) were collected, on average, from 5 ± 2 (Galician coastal upwelling), 7 ± 1 (NW Mediterranean) and 11 ± 2 (tropical and subtropical Atlantic Ocean) depths in rinsed polyethylene tubes and stored frozen at -20°C until analysis on land, according to standard methods using the automated colorimetric technique (Grasshoff et al., 2007). The frequency histogram of sampling depths collected for the determination of nitrate concentration in each region is indicated in Figure A2-A in the Supplementary material, whereas the maximum sampling depth where the microstructure turbulence profiler was deployed is indicated in Table 1.

2) DENSITY AND NITRATE RELATIONSHIPS The authors also mention that for some of the stations nutrient data was not available, and instead of nutrient bottle data, a relationship between density and nitrate was used. Again it is not clear how robust the relationship between nitrate concentration and density was for the relevant stations. Could the authors provide supplementary plots of the nutrient versus density relationship that was used to estimate nitrate gradients, similar to that of Williams et al. (2013a GRL 40:5467-5472; 2013b Limnol. Oceanogr.: Fluids and Envs 3:61-73)?

C3

Only in one station sampled in the Galician coastal upwelling ecosystem during the NICANOR project observations of nutrient concentration were not available. Instead nitrate concentration was computed from a nitrate-density (σ_t) relationship built by using all samples ($n=52$) collected during the NICANOR sampling period. A new figure (Figure A2-B) has been included in the supplementary material to show this relationship. The relationship showed a linear behavior ($\text{NO}_3 = 9.7788 \cdot \sigma_t - 256.38$; $r = 0.930$; $p < 0.001$) for density ranging between 26.1 and 27.1 kg m^{-3} .

Original: Page 5 – Line 13-14 In those stations carried out during the NICANOR cruises, where nitrate concentrations were not available, they were obtained by using nitrate-density relationships (Moreira-Coello et al., 2017)

Change: Page 5 – Line 26-29 In one station carried out during the NICANOR cruise, where nitrate concentrations were not available, these were obtained by using a nitrate-density relationship built by using all samples ($n=52$) collected during the NICANOR sampling period. The relationship showed a linear behavior ($\text{NO}_3 = 9.7788 \cdot \sigma_t - 256.38$; $\text{Adj-}r^2 = 0.87$; $p < 0.001$) for density ranging between 26.1 and 27.1 kg m^{-3} (Figure A2-B).

3) EPISODIC NATURE OF MIXING Mixing events in some regions can be episodic, yet short-term vertical pulses of nutrients can trigger significant shifts in community structure. In some oceanic regions tidal mixing can also be important. The authors mention that 3-10 profiles were taken, but it would also be helpful to know the time interval over which these profiles were made and how this varied between the three study regions (again a frequency histogram documenting this would be helpful). Could it be that for some regions the flux of nutrients could be significantly underestimated given that such short-term events may not be captured in MSS profile data? Given the general audience of the journal, both the strengths and shortcomings of this method of estimating nutrient supply should be provided.

We completely agree with the reviewer that episodic bursts of turbulence can induce

C4

episodic inputs of nutrient supply which can be easily missed in sets of 2-10 profiles. The microstructure turbulence profiles used for computing nitrate fluxes at each station were always deployed successively. Sets include 2-11 in the tropical and subtropical Atlantic (37 ± 18 min), 6-7 in the NW Mediterranean (76 ± 22 min) and 3-402 in the Galician coastal upwelling (65 ± 246 min). Our dataset includes two high-frequency samplings carried out in the outer part of Ría de Vigo (Galician upwelling ecosystem) in August 2013 (CHAOS cruises). During these cruises two 25-hour series of turbulent microstructure and currents observations were carried out during spring and neap tides. Turbulent kinetic energy dissipation at the interface between upwelled and surface waters was enhanced by two orders of magnitude during the ebbs, as the result of the interplay of the bi-directional upwelling circulation and the tidal currents shear (Fernández-Castro et al., 2018). This mechanism could have important implications for the functioning of biological processes, as it can act as a pathway for nutrient supply from upwelled nutrient-rich deep waters into the sunlit surface waters. In fact, diffusive nitrate fluxes due to the enhanced dissipation observed during CHAOS-springs, could be responsible for about half of the phytoplankton primary production estimated in this system during periods of upwelling relaxation-stratification (Villamaña et al., 2017). A new figure included in the supplementary material (Figure A2-C) indicates the number of turbulent profiles deployed at each station for each region. The duration of the microstructure turbulent profiler operation is indicated in Table 1 and the text has been modified to:

Original: Page 4 Line 28-29 Measurements of dissipation rates of turbulent kinetic energy (ε) were conducted at 3-10 profiles for each station to the bottom, or 300 m over deep waters.

Change:Page 4 Line 26- Page 5 Line 5 Measurements of dissipation rates of turbulent kinetic energy (ε) were conducted to the bottom, or to 137-323 m over deep waters (see Table 1). The microstructure turbulence profiles used for computing nitrate fluxes at each station were always deployed successively. Sets include 2-11 in the tropical

C5

and subtropical Atlantic (operation time 37 ± 18 min), 6-7 in the NW Mediterranean (76 ± 22 min) and 3-402 in the Galician coastal upwelling (65 ± 246 min) (Figure A2-C).

Bursts of turbulence can induce episodic inputs of nutrient supply which can be easily missed in sets of low number of profiles. In coastal regions where short-term variability of mixing processes is expected to be higher, our dataset includes two high-frequency samplings carried out in the outer part of Ría de Vigo (Galician upwelling ecosystem) in August 2013 (CHAOS cruises). During these cruises two 25-hour series of turbulent microstructure and currents observations were carried out during spring and neap tides. Turbulent kinetic energy dissipation at the interface between upwelled and surface waters was enhanced by two orders of magnitude during the ebbs, as the result of the interplay of the bi-directional upwelling circulation and the tidal currents shear (Fernández-Castro et al., 2018).

4) PICOPHYTOPLANKTON BIOMASS The authors report the estimates of picophytoplankton biomass and ratios of biomass, but I was unable to find how the authors convert from cell abundance to carbon per unit volume. This is quite important, as there are several group-specific carbon conversion factors in the literature and for the larger eukaryotic cells it is likely a biovolume conversion factor may provide a better estimate, as the size range within this subgroup can be significant.

We thank the reviewer for pointing out that this information was missing. In order to estimate biovolume (BV), we used an empirical calibration between Size Scatter (SSC) and cell diameter (Calvo-Díaz and Morán, 2006), assuming spherical shape for all groups. The following volume-to-carbon conversion factors were used for picotrophic groups: $230 \text{ fg C} \cdot \text{BV}$ for *Synechococcus*, $240 \text{ fg C} \cdot \text{BV}$ for *Prochlorococcus* and $237 \text{ fg C} \cdot \text{BV}$ for picoeukaryotes (Worden et al., 2004). For bacteria BV was converted into carbon biomass by using the allometric relationship: $108.8 \text{ fg C} \cdot \text{BV}^{0.898}$ (Gundersen et al., 2002).

Original: Page 6 Line 19-24 Autotrophic cells were separated into two groups of

C6

cyanobacteria (*Synechococcus* and *Prochlorococcus*) and one group of small picoeukaryotes, based on their fluorescence and light scatter signals (SSC), as explained in Calvo-Díaz et al. (2006). Two groups of heterotrophic prokaryotes (LNA and HNA) were distinguished based on their relative green fluorescence, which was used as a proxy for nucleic acid content (Gasol and del Giorgio, 2000; Bouvier et al., 2007).

Change: Page 7 Line 4-15 Autotrophic cells were separated into two groups of cyanobacteria (*Synechococcus* and *Prochlorococcus*) and one group of small picoeukaryotes, based on their fluorescence and light scatter signals (SSC), as explained in Calvo-Díaz et al. (2006). Two groups of heterotrophic prokaryotes (LNA and HNA) were distinguished based on their relative green fluorescence, which was used as a proxy for nucleic acid content (Gasol and del Giorgio, 2000; Bouvier et al., 2007). In order to estimate biovolume (BV), we used an empirical calibration between Size Scatter (SSC) and cell diameter (Calvo-Díaz et al., 2006), assuming spherical shape for all groups. The following volume-to-carbon conversion factors were used for picotrophic groups: 230 fg C for *Synechococcus*, 240 fg C for *Prochlorococcus* and 237 fg C for picoeukaryotes (Worden et al., 2004). For bacteria BV was converted into carbon biomass by using the allometric relationship: $108.8 \text{ fg C} \cdot \text{BV}^{0.898}$ (Gundersen et al., 2002). More details about the processing and analysis of flow cytometry samples are provided in Calvo-Díaz et al. (2006, TRYNITROP), Gomes et al. (2015, FAMOSO), Villamaña et al. (2017, CHAOS) and Moreira-Coello et al. (2017, NICANOR). Abundance data obtained at different depths for each station were combined to compute depth-integrated biomass for the photic layer.

5) EXTRAPOLATION TO THE GLOBAL OCEAN I was surprised to see that over half of the stations used were from coastal embayments. One could argue from many points of view that these regions may not be representative of the open-ocean eutrophic environments (likely different taxonomic diversity within these gross cytometric groupings, potential supply of nutrients from terrigenous sources, different light environment caused by attenuation by CDOM and sediments, need to correct for advective

C7

flux). Perhaps the authors have supporting literature/data that would help convince the reader that these embayments broadly reflect the environmental conditions of offshore stations, but even with such supporting information they should also highlight the need for data from open-ocean meso- and eutrophic environments that would help further resolve the global relationship between mixing and picoplankton community structure.

We agree with this reviewer that a larger data set including a wider range of conditions will be desirable. However, please note that the Galician Rías, despite being in general longer and narrower than many open bays in upwelling areas (e.g., Monterey Bay in California, False Bay in South Africa, Antofagasta Bay in Chile, and Todos Santos Bay in Mexico), they resemble them in that its primary hydrographic and circulation features are determined by the extension of wind-driven flow on the external continental shelf throughout the bay (Alvarez-Salgado et al., 2010). Fertilization in the Rías occurs essentially by coastal upwelling, being fresh and rain water inputs residual (2

Original Page 5 Line 21-25 Most stations carried out in the Galician coastal upwelling were conducted inside three different Rías (Ría de Vigo, Ría de Pontevedra and Ría de A Coruña). The Rías are coastal embayments affected by seasonal wind-driven coastal upwelling of cold, nutrient-rich North Atlantic Central water (Wooster et al., 1976; Fraga, 1981; Álvarez-Salgado et al., 1993). The total nitrate supply in the Galician Rías was computed as the sum of nitrate vertical diffusion plus nitrate vertical advection due to coastal upwelling.

Modify Page 6 Line 5 - 12

Most stations carried out in the Galician coastal upwelling were conducted inside three different Rías (Ría de Vigo, Ría de Pontevedra and Ría de A Coruña). The Rías are coastal embayments affected by seasonal wind-driven coastal upwelling of cold, nutrient-rich North Atlantic Central water (Wooster et al., 1976; Fraga, 1981; Álvarez-Salgado et al., 1993). The Galician Rías, despite being in general longer and narrower than many open bays in upwelling areas, they resemble them in that its primary hydro-

C8

graphic and circulation features are determined by the extension of wind-driven flow on the external continental shelf throughout the bay (Alvarez-Salgado et al., 2010). Fertilization in the Rías occurs essentially by coastal upwelling, being fresh and rain water inputs residual (2

The dataset is largely confined to a specific geographic region (40N-30S, covering a limited number of biochemical provinces in the Atlantic Basin), yet the authors use relationships from this study to predict future changes in picoplankton community structure across the entire globe. Would the authors consider limiting their predictions of future community structure to the geographic regions/ latitudinal gradients that are used to develop the predictive models? Given that the global ocean covers a variety of biogeochemical regimes, some of which may not be limited by nitrate, restricting the geographical scope of the future predictions may be advisable, even though the overall patterns tend to broadly resemble those from other global studies.

Following the comments by both reviewers this section has been deleted from the manuscript.

6) USE OF MOREL MODEL TO ESTIMATE DEPTH OF PHOTIC LAYER Is the light attenuation observed in the Galician coastal stations largely a result of phytoplankton or other optically-active substances? I mention this because the model of Morel used to estimate euphotic depth is restricted to Case-1 (open ocean) waters where light attenuation is dominated by phytoplankton.

As mentioned above primary hydrographic and circulation features in the Galician Rías are determined by the extension of wind-driven flow on the external continental shelf throughout the bay. Note that light attenuation is exclusively used in the manuscript to get an estimate of the base of the euphotic layer, to be used as the lower limit to compute depth-integrated biomass. Using water type 2 equations would result in a shallower limit for the euphotic layer, which could miss phytoplankton biomass sometimes located deeper than this limit in this system (see Figure 1 in Cermeño et al., (2016)). In

C9

our study the Morel equation was only used to compute light attenuation coefficients during the NICANOR, ASIMUTH and CHAOS cruises, which sampled stations in the outer part of the Rías. This information is now clarified in the methods section. A new figure (Figure A2-D) has been also included in the supplementary material to compare the base of the euphotic zone, as derived from PAR data and the Morel equation, by using data collected during the HERCULES cruises.

Original Pag 4 Line 20-24 For those cruises where PAR profiles were not available (ASIMUTH, CHAOS and NICANOR), the depth of the photic layer was calculated by considering light attenuation coefficients derived from surface chlorophyll-a data estimated from the space, following the algorithms proposed by Morel et al. (2007) (<http://globcolour.info>).

Modified Pag 4 Line 17-22 For those cruises where PAR profiles were not available (ASIMUTH, CHAOS and NICANOR), which sampled stations in the outer part of the Rías, the depth of the photic layer was calculated by considering light attenuation coefficients derived from surface chlorophyll-a data, following the algorithms proposed by Morel et al. (2007) for Case-1 waters ($\log_{10}Z_{eu}=1.524 - 0.460[\text{Chl}]_{\text{surf}} - 0.00051[\text{Chl}]_{\text{2surf}} + 0.0282[\text{Chl}]_{\text{3surf}}$). A comparison of the estimation of the base of the euphotic zone by using the Morel et al equation and the data collected by a radiometer during the HERCULES cruise is shown in Figure A2-D.

Interactive comment on Biogeosciences Discuss., <https://doi.org/10.5194/bg-2018-211>, 2018.

C10

Table 1. Details of the data included in this study. Domain referred to the tropical and subtropical Atlantic ocean (T), the Northwestern Mediterranean Sea (M), and the Galician coastal upwelling (G). N indicates the number of stations sampled at each cruise. Duration (mean \pm standard deviation) is the time duration in minutes of the turbulence profiler deployment in each station. Duration (mean \pm standard deviation, in minutes) is the time used for the microstructure turbulence operation at each station). Depth (mean \pm standard deviation, in meters) is the maximum depth reached by the microstructure profiler.

Domain	Region	N	Cruise	Vessel	Date	Duration	Depth
T	NE Atlantic	8	CARPOS	Hespérides	14/10/06- 22/11/06	57 \pm 24	137 \pm 15
T	Atlantic	18	TRYNITROP	Hespérides	14/04/08 - 02/05/08	45 \pm 12	219 \pm 19
M	Liguro-Provençal Basin	6	FAMOSO I	Sarmiento de Gamboa	14/3/09 - 22/3/09	66 \pm 5	259 \pm 38
M	Liguro-Provençal Basin	10	FAMOSO II	Sarmiento de Gamboa	30/4/09 - 13/05/09	94 \pm 4	273 \pm 2
M	Liguro-Provençal Basin	3	FAMOSO III	Sarmiento de Gamboa	16/09/09 - 20/09/09	133 \pm 3	323 \pm 24
G	Ría de A Coruña	1	HERCULES I	Lura	07/06/10	20 \pm 4	35 \pm 2
G	Ría de A Coruña	5	HERCULES II	Lura	28/09/11 - 29/09/11	11 \pm 8	33 \pm 26
G	Ría de A Coruña	13	HERCULES III	Lura	16/07/12 - 20/07/12	8 \pm 5	41 \pm 29
G	Ría de Vigo	9	DISTRAL	Mytilus	14/02/12 - 06/11/12	110 \pm 76	38 \pm 1
G	Ría de Vigo	2	CHAOS	Mytilus	20/08/13 - 27/08/13	1515 \pm 6	41 \pm 29
G	Ría de A Coruña	12	NICANOR	Lura	27/02/14 - 17/12/15	33 \pm 5	62 \pm 3
G	Rías de Vigo & Pontevedra	10	ASIMUTH	Ramón Margalef	17/06/13 - 21/06/13	10 \pm 4	28 \pm 10

Fig. 1. Table 1

C11

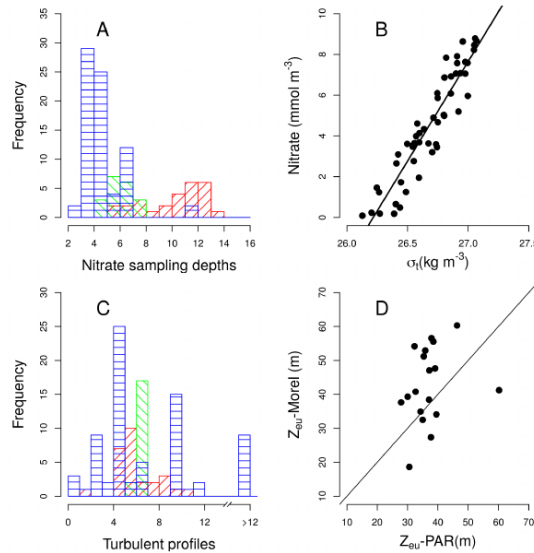


Figure A2. A) Frequency histograms of the number of nutrient where samples for nitrate concentration were collected at each station and domain: tropical and subtropical Atlantic ocean (red), the Northwestern Mediterranean (green) and Galician coastal upwelling (blue). B) Pair scatter plot representing the relationship between nitrate concentration and density built by using all samples collected during the NICANOR sampling period. C) Frequency histogram of the number of turbulence profiles deployed at each station and domain. D) Pair scatter plot representing the relationship between the euphotic zone depth (Z_{eu}) computed using the Morel et al. (2007) equation and the data collected by a radiometer during the HERCULES cruise measured used a radiometer and predicted using the relationship with surface chlorophyll Morel et al. (2007), the solid line represents 1:1 relationship.

Fig. 2. Figure A2

C12

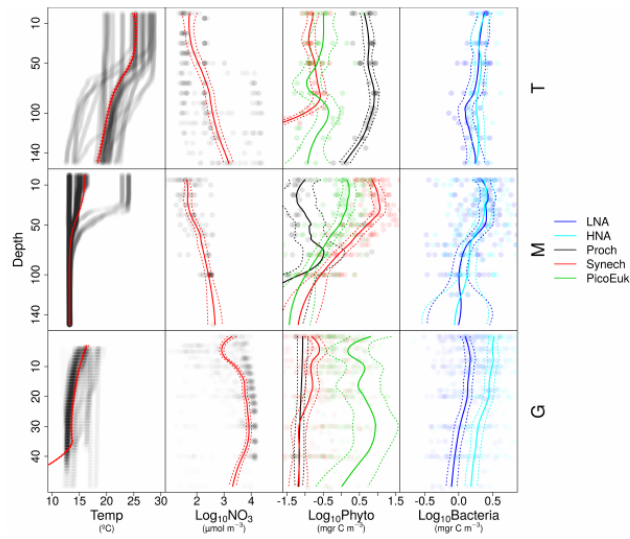


Figure A3. Vertical distribution of temperature (Temp), nitrate (NO_3) and picoplankton biomass of autotrophic (Phyto) and heterotrophic (Bacteria) groups for each domain: tropical and subtropical Atlantic ocean (T), the Northwestern Mediterranean (M), and Galician coastal upwelling (G). Points represent raw data and the solid line the locally weighted scatterplot smoothing (LOESS). Dashed lines indicate 95% confidence intervals. Dot and line color intensity indicates the number of overlapping observations.

Fig. 3. Figure A3